Accurate Measurements of Long-Range Heteronuclear Coupling Constants from Homonuclear 2D NMR Spectra of Isotope-Enriched Proteins

GAETANO T. MONTELIONE,* MARJORIE E. WINKLER,† PETER RAUENBUEHLER,†
AND GERHARD WAGNER*

*Biophysics Research Division, The University of Michigan, Ann Arbor, Michigan 48109,
and †Department of Medicinal and Biomolecular Chemistry, Genentech, Inc., 460 Point San Bruno Blvd.,
South San Francisco, California 94080

Long-range heteronuclear coupling constants are of high interest for studies of protein structure and dynamics. Today, typical sets of conformational constraints for protein structures consist of a large number of NOE constraints and a small number of dihedral angle constraints on ϕ and χ^1 obtained from homonuclear proton–proton coupling constants. The resultant structures show well-defined overall polypeptide folds. However, local backbone structures are not determined as precisely as may be possible with additional data. Furthermore, many side chains are less well defined than the backbone. While amino acid side chains may often adopt multiple conformations, there are no good approaches for characterizing their distributions in proteins.

Measurements of heteronuclear coupling constants would provide a whole new class of constraints that could significantly improve protein structures at the local level, where improvement is needed most. The most promising approach is to measure $^{15}N-^1H$ vicinal coupling constants. This would lead to the following achievements. (i) Measurements of the coupling constants between the peptide nitrogen and the β-protons, combined with measurements of homonuclear coupling constants between α- and β-protons, can provide a characterization of the side-chain dihedral angle χ^1 and stereospecific assignments of β-methylene protons. For mobile side chains, these data can also be used to determine distributions of rotamer populations. This approach is an improvement over previous strategies which have used homonuclear coupling constants and NOEs to achieve stereospecific assignments (1). (ii) Stereospecific assignments of β-methylene proton resonances, in turn, would provide a more precise interpretation of intraresidue H^N-H^β and sequential $H^\beta-H^N$ NOEs, which depend on the values of the intervening dihedral angles ϕ, χ^1 and χ^1, ψ, respectively. (iii) Measurements of the coupling constants between the α-proton of residue i and the peptide nitrogen of residue $i + 1$, combined with sequential NOEs, should provide improved determinations of the backbone dihedral angle ψ_i. (iv) Vicinal couplings between methylene protons and side-chain amide or guanido nitrogens could also provide Asn χ^2, Gln χ^3, and Arg χ^4 dihedral angle constraints.

198

These motivations for measuring ^{15}N–^{1}H coupling constants have long been recognized. However, it has been difficult to measure heteronuclear coupling constants accurately from NMR spectra of proteins. When the coupling constants must be measured from the multiplet structures of cross peaks in 2D heteronuclear correlation spectra the measurements are biased by cancellation or summation effects of cross-peak components (2). In addition, such experiments suffer from poor sensitivity at natural abundance ^{15}N and are often difficult to phase. Until now, only the sensitivity problem has been solved, using technologies for uniform ^{15}N enrichment of proteins.

This paper describes our simple approach for measuring ^{15}N–^{1}H coupling constants in uniformly ^{15}N-enriched proteins. We record homonuclear 2D ^{1}H NMR spectra (e.g., NOESY, ROESY, RELAY, or TOCSY) that contain cross peaks between the protons directly bound to ^{15}N and the protons for which the long-range coupling to that same nitrogen should be measured. Especially useful are cross peaks between amide protons and the β-protons of the same residue (to characterize χ^1) or cross peaks between the α-protons of residue i and the amide protons of residue $i + 1$ (to characterize ψ). Since we do not pulse the ^{15}N nucleus the cross peaks show E.COSY-type multiplet structures where the heteronuclear couplings are passive. They are split in one dimension by the large direct heteronuclear coupling and, in the other dimension, by the small long-range heteronuclear coupling of interest. The large direct splitting provides good resolution of the cross-peak components and allows accurate measurements of both heteronuclear coupling constants. We use the cross peak for which the larger direct splitting is along ω_1 and the smaller long-range coupling is along ω_2 to take advantage of the higher resolution along the latter dimension. As in homonuclear E.COSY, the sign of the long-range coupling relative to the direct heteronuclear coupling can be determined. Similar effects have been reported previously for ^{113}Cd-enriched metallothionein-2 (3).

As an example of this approach, we have used NOESY to measure long-range heteronuclear coupling constants in uniformly ^{15}N-enriched type α human transforming growth factor (hTGFα). TGFα is a small protein containing 50 amino acid residues and three disulfide bonds. The cloned protein is expressed in *Escherichia coli* (4, 5). Its small size and biological importance make hTGFα an ideal system in which to develop approaches for protein structure determination and molecular design. For this reason, we have recently determined a nearly complete set of sequence-specific proton resonance assignments and have characterized the secondary structure of hTGFα using conventional homonuclear 2D NMR methods (6). The refinement of the three-dimensional structure of hTGFα will be aided greatly by measurements of heteronuclear ^{15}N–^{1}H coupling constants.

Uniformly ^{15}N-enriched hTGFα was prepared by growing the *E. coli* expression system in a totally synthetic media containing (^{15}NH$_4$)$_2$SO$_4$ as the major nitrogen source. The region of cross peaks between the amide protons (along ω_1) and the aliphatic protons (along ω_2) of a NOESY spectrum of 99% ^{15}N-enriched hTGFα in H$_2$O solvent is shown in Fig. 1. Each NOESY cross peak involving an H^N proton is split into two components in the ω_1 dimension due to $^1J(^{15}$N–H). Many also show measurable displacements in ω_2 arising from vicinal ^{15}N–^{1}H coupling. The patterns of these cross peaks show that the vicinal ^{15}N–^{1}H couplings have the same sign as the direct ^{15}N–^{1}H couplings because the low-field component along ω_1 is also the low-
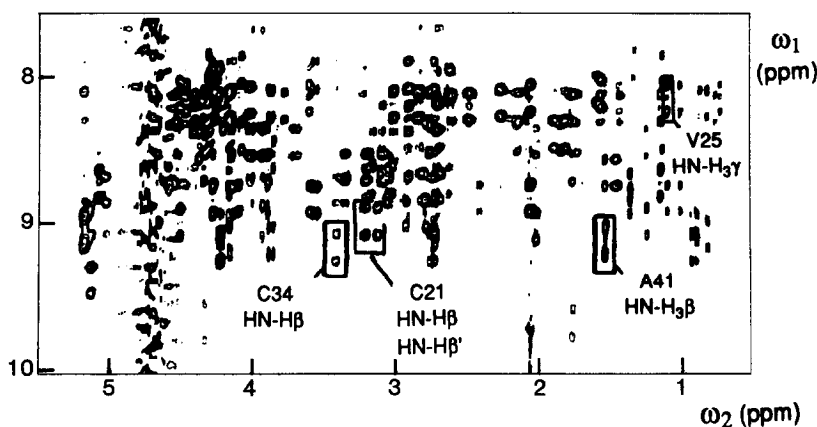
FIG. 1. Expansion of a ^{1}H-NOESY spectrum of 99% ^{15}N-enriched hTGFα in 90% H_2O/10% ^2H_2O solvent, protein concentration about 5 mM, pH 3.5, temperature 30°C, and mixing time 350 ms. The cross peaks between the H^N and aliphatic protons are shown. The digital resolutions are 12.6 and 1.0 Hz/pt in ω_1 and ω_2, respectively.

field component along ω_2. Since it is known that these direct ^{15}N–^{1}H couplings are negative (7), the vicinal ^{15}N–^{1}H couplings must also be negative. Expansions of representative examples are shown in Figs. 2 and 3.

Long-range heteronuclear coupling constants were determined by measuring the displacements of resonance peaks in ω_2 cross sections. The precision of our measurements is determined both by the digital resolution of the transformed spectra (1.0 Hz/pt in ω_2) and by our ability to identify the centers of the displaced cross-peak components. Measurements made from several cross sections of the same cross peak indicate a reliability of about ±0.5 Hz. Approaches for improving this precision will be presented elsewhere.

Representative H^N–H^β cross peaks bearing conformational information of interest are shown in Fig. 2. For Cys-34 the ensemble-averaged $^3J(^{15}N–H^\beta)$ coupling to the downfield H^β proton is −5.5 ± 0.5 Hz (Fig. 2A), corresponding to a trans orientation of these two atoms (8). Information is not yet available for the upfield H^β proton owing to partial overlap of this cross peak. For Cys-21, both H^N–H^β cross peaks are resolved (Fig. 2B) with $^3J(^{15}N–H^\beta)$ values of −1.3 ± 0.5 and −1.8 ± 0.5 Hz for the downfield and upfield resonances, respectively. These measurements indicate (8) that both protons are gauche with respect to the ^{15}N atom; i.e., the corresponding dihedral angle χ^1 is about 180°.

In order to evaluate the accuracy of these measurements, we have determined the $^3J(^{15}N–H^\beta)$ coupling constants for well-resolved intraresidue H^N–H^β_3 cross peaks of Ala-41 and Ala-46. For an alanine side chain it is reasonable to assume equally populated staggered rotamer states for the methyl protons. The corresponding ensemble-averaged $^3J(^{15}N–H^\beta)$ coupling constants calculated from different published calibrations of the Karplus curve (8–10) range from −2.1 to −2.9 Hz, in good agreement with our measured values of −2.4 ± 0.5 Hz for both Ala-41 (Fig. 3A) and Ala-46 (not shown). As an additional check for systematic errors, we also examined some
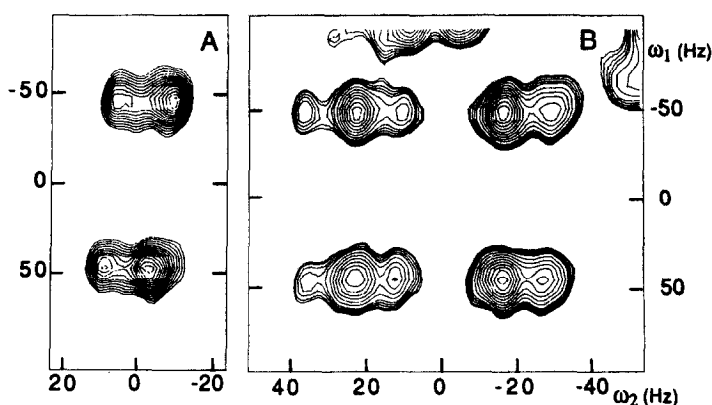
FIG. 2. Expansions of cross peaks involving methylene resonances from the NOESY spectrum of Fig. 1. (A) Intraresidue H^N–H^β cross peak of Cys-34 manifesting an ω_2 displacement due to vicinal $^3J(^{15}N$–$H^\beta)$ heteronuclear coupling of -5.5 ± 0.5 Hz. (B) Both intraresidue $^3J(^{15}N$–$H^\beta)$ cross peaks of Cys-21, manifesting heteronuclear couplings of -1.3 ± 0.5 and -1.8 ± 0.5 Hz, respectively. These measurements indicate an ensemble-averaged dihedral angle χ^1 of about 180°.

cross peaks in which the H^N proton is coupled to ^{15}N but the aliphatic proton is not, e.g., the intraresidue H^N–H^γ_3 NOESY cross peak of Val-25 (Fig. 3B). These cross peaks show no displacement in the ω_2 dimension.

In principle the approach described in this paper can also be used to measure vicinal $^3J(H^\alpha$–$^{15}N)$ couplings as displacements in interresidue H^α–H^N NOESY cross peaks. These coupling constants depend on the backbone dihedral angle ψ and are proposed to range from about 0 to -5 Hz (7, 11, 12). While only a few H^α–H^N NOESY cross peaks for hTGFα are sufficiently well resolved to be useful in these measurements, none of these have $^3J(H^\alpha$–$^{15}N)$ splittings large enough to be mea-
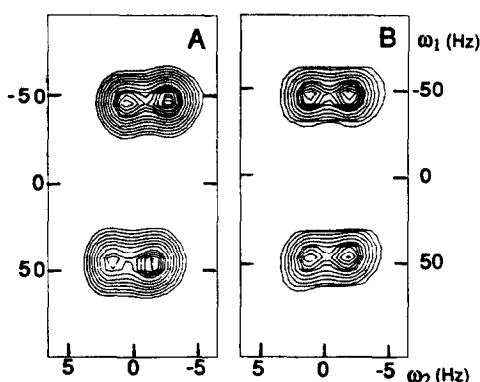

FIG. 3. Expansions of cross peaks involving methyl resonances from the NOESY spectrum of Fig. 1. (A) Intraresidue H^N–H^δ_3 cross peak of Ala-41. The displacement along ω_2 is due to the vicinal $^3J(^{15}N$–$H^\beta)$ heteronuclear coupling constant of -2.4 ± 0.5 Hz. (B) Intraresidue H^N–H^γ_3 cross peak of Val-25 showing no long-range heteronuclear coupling.

sured. They are all smaller than about 1 Hz. Similar observations have been reported for ^{15}N-enriched peptides (8, 13).

To illustrate the physical basis of this method, we have used product operator formalism (14) to simulate an intraresidue H^N–H^β NOESY cross peak of the ^{15}N-enriched amino acid spin system shown in Fig. 4. We considered the NOESY peak at $\omega_1 = \Omega_{HN}$ and $\omega_2 = \Omega_{H\beta}$ for which the magnetization begins on the H^N proton. The relevant terms of the product operator at the end of the evolution period are

$$-I_y\cos(\Omega_I t_1)\cos(\pi J_1 t_1)\cos(\pi J_2 t_1) + 2I_y K_z\sin(\Omega_I t_1)\sin(\pi J_1 t_1)\cos(\pi J_2 t_1) \quad [1]$$

in which $J_1 \equiv {}^1J(^{15}$N–H$)$, $J_2 \equiv {}^3J($HN–H$^\alpha)$, and I and K refer to the H^N proton and ^{15}N nuclei, respectively. The additional terms which are not shown are eliminated by standard NOESY phase cycles. The second proton pulse of the NOESY sequence converts the in-phase and antiphase terms of Eq. [1] into longitudinal magnetization
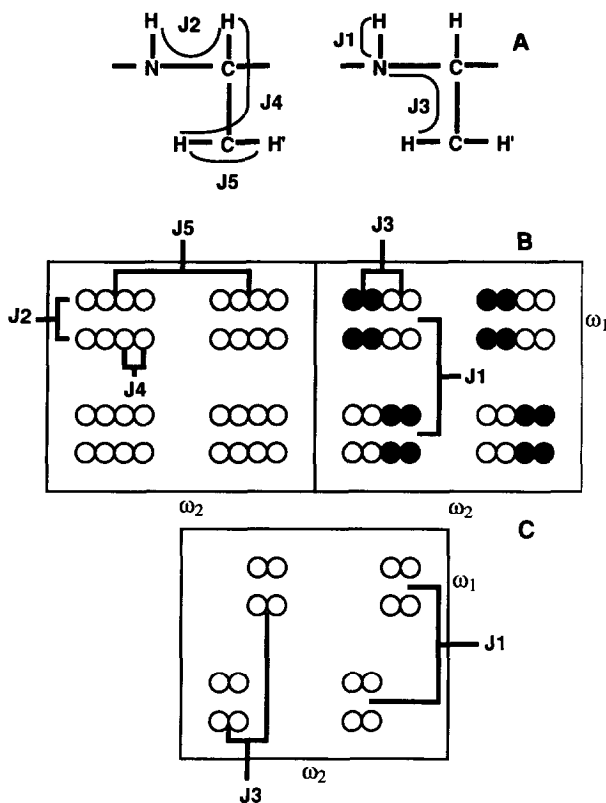

FIG. 4. Schematic drawing of a simulated H^N–H^β NOESY cross peak for an ^{15}N-enriched protein. (A) A simple amino acid spin system showing the homonuclear (left) and heteronuclear (right) spin coupling constants used for the cross-peak simulation. The relevant coupling constants J_1, J_2, J_3, J_4, and J_5 are defined in the text. In this simulation, $J_1 > J_5 > J_2 = J_3 > J_4$ and the product $J_1 \times J_3 > 0$. (B) Contributions to cross-peak fine structure arising from longitudinal magnetization transfer I_z to M_z (left) and from transfer of heteronuclear two-spin order $I_z K_z$ to $M_z K_z$ (right) during the NOESY mixing time τ_m. (C) Superposition of these two components.

(I_z) and two-spin order ($I_z K_z$), respectively. Because the ^{15}N nuclei are not affected by this second proton pulse, the K_z components of the product operator remain aligned along the z axis. Nuclear Overhauser effects between the H^N and the H$^\beta$ protons during the mixing period next convert longitudinal magnetization and two-spin order of the H^N proton into the corresponding states of the H$^\beta$ proton. Ignoring the diagonal peaks and considering only the magnetization on the y axis, the observable terms of the final two-dimensional product operator are

$$-M_y\cos(\Omega_I t_1)\cos(\Omega_M t_2)\cos(\pi J_1 t_1)\cos(\pi J_2 t_1)\cos(\pi J_3 t_2)\cos(\pi J_4 t_2)\cos(\pi J_5 t_2)$$

$$-M_y\sin(\Omega_I t_1)\sin(\Omega_M t_2)\sin(\pi J_1 t_1)\cos(\pi J_2 t_1)\sin(\pi J_3 t_2)\cos(\pi J_4 t_2)\cos(\pi J_5 t_2)$$

$$[2]$$

in which $J_3 \equiv {}^3J(^{15}\text{N-H}^\beta)$, $J_4 = {}^2J(\text{H}^\beta\text{-H}^{\beta'})$, $J_5 \equiv {}^3J(\text{H}^\alpha\text{-H}^\beta)$, and M denotes the H$^\beta$ spin. The first term of Eq. [2] is the usual in-phase homonuclear NOESY cross peak, while the second term, arising from heteronuclear two-spin order during the mixing time, is a superimposed NOESY cross peak which is in-phase with respect to all of the homonuclear couplings and antiphase in t_1 and t_2 relative to $^1J(^{15}\text{N-H})$ and $^3J(^{15}\text{N-H}^\beta)$, respectively. This second pathway of magnetization is converted back into observable magnetization only if the two protons associated with the NOESY cross peak are coupled to the same ^{15}N nucleus (or in the special case of simultaneous ^{1}H-^{1}H and ^{15}N-^{15}N incoherent magnetization transfer). The cross-peak fine structures resulting from each of the two terms of Eq. [2], and their superposition, are shown in Fig. 4.

The primary limitation of the approach described here is overlap between NOESY cross peaks. Many of the NOESY cross peaks of ^{15}N-enriched hTGFα have one or both components overlapped with other peaks, complicating their interpretation in terms of coupling constants. In this respect, the TOCSY and RELAY-COSY versions of the experiment, which contain fewer cross peaks, are advantageous. Improved resolution could perhaps be obtained best by introducing a third heteronuclear frequency domain. This could be achieved by combining ^{15}N-^{1}H heteronuclear-correlated and homonuclear TOCSY, RELAY-COSY, ROESY, or NOESY pulse sequences into heteronuclear 3D NMR experiments (15, 16).

The results presented in this Communication demonstrate a simple approach for measuring long-range heteronuclear couplings in ^{15}N-enriched proteins. This information can be combined with proton–proton coupling constants to determine β-methylene prochirality assignments, ensemble-averaged values of side-chain (e.g., χ^1) dihedral angles, and dynamic distributions of side-chain rotamer states (13, 17–19). Such information will be especially useful for refining protein structures and for characterizing subtle conformational changes which may accompany single-site mutations.

ACKNOWLEDGMENTS

REFERENCES

1. S. G. HYBERTS, W. MÄRKI, AND G. WAGNER, *Eur. J. Biochem.* **164**, 625 (1987).
2. D. NEUHAUS, G. WAGNER, M. VASAK, J. H. R. KÄGI, AND K. WÜTHRICH, *Eur. J. Biochem.* **151**, 257 (1985).
3. D. NEUHAUS, G. WAGNER, M. VASAK, J. H. R. KÄGI, AND K. WÜTHRICH, *Eur. J. Biochem.* **143**, 659 (1984).
4. R. DERYNCK, A. B. ROBERTS, M. E. WINKLER, E. Y. CHEN, AND D. V. GOEDDEL, *Cell* **38**, 287 (1984).
5. M. E. WINKLER, T. BRINGMAN, AND B. J. MARKS, *J. Biol. Chem.* **261**, 13,838 (1986).
6. G. T. MONTELIONE, M. E. WINKLER, L. E. BURTON, E. RINDERKNECHT, M. B. SPORN, AND G. WAGNER, *Proc. Natl. Acad. Sci. USA,* in press.
7. V. F. BYSTROV, *Prog. NMR Spectrosc.* **10**, 41 (1976).
8. A. DEMARCO, M. LLINAS, AND K. WÜTHRICH, *Biopolymers* **17**, 2727 (1978).
9. R. L. LICHTER AND J. D. ROBERTS, *J. Org. Chem.* **35**, 2806 (1970).
10. J. A. SOGN, W. A. GIBBONS, AND E. W. RANDALL, *Biochemistry* **12**, 2100 (1973).
11. M. BARFIELD AND H. L. GEARHART, *Mol. Phys.* **27**, 899 (1974).
12. V. F. BYSTROV, YU. D. GAVRILOV, AND V. M. SOLKAN, *J. Magn. Reson.* **19**, 123 (1975).
13. E. R. STIMSON, Y. C. MEINWALD, G. T. MONTELIONE, AND H. A. SCHERAGA, *Int. J. Pept. Protein Res.* **27**, 569 (1986).
14. O. W. SØRENSEN, G. W. EICH, M. H. LEVITT, G. BODENHAUSEN, AND R. R. ERNST, *Prog. NMR Spectrosc.* **16**, 163 (1983).
15. C. GRIESINGER, O. W. SØRENSEN, AND R. R. ERNST, *J. Am. Chem. Soc.* **109**, 7227 (1987).
16. S. W. FESIK AND E. R. P. ZUIDERWEG, *J. Magn. Reson.* **78**, 588 (1988).
17. A. J. FISCHMAN, H. R. WYSSBROD, W. C. AGOSTA, AND D. COWBURN, *J. Am. Chem. Soc.* **100**, 54 (1978).
18. A. J. FISCHMAN, D. H. LIVE, H. R. WYSSBROD, W. C. AGOSTA, AND D. COWBURN, *J. Am. Chem. Soc.* **102**, 2533 (1980).
19. H. KESSLER, C. GRIESINGER, AND K. WAGNER, *J. Am. Chem. Soc.* **109**, 6927 (1987).